

# Fabrication of Sub-Micron Surface Structures on Copper, Stainless Steel and Titanium using Picosecond Laser Interference Patterning

Matthias Bieda<sup>a</sup>, Mathias Siebold<sup>b</sup>, Andrés Fabián Lasagni<sup>a, c</sup>

<sup>a</sup> Fraunhofer-Institut für Werkstoff- und Strahltechnik (IWS), Winterbergstr. 28, 01277 Dresden, Germany

<sup>b</sup> Helmholtz-Zentrum Dresden-Rossendorf (HZDR), Bautzner Landstr. 400, 01328 Dresden, Germany, Email: m.siebold@hzdr.de

<sup>c</sup> Technische Universität Dresden, Institut für Fertigungstechnik, 01062 Dresden, Germany, Email: andres\_fabian.lasagni@tu-dresden.de

Corresponding author:

Matthias Bieda

Fraunhofer Institut für Werkstoff- und Strahltechnik IWS

Winterbergstraße 28, 01277 Dresden, Germany

Email: matthias.bieda@iws.fraunhofer.de

## Abstract

Picosecond direct laser interference patterning (ps-DLIP) is investigated theoretically and experimentally for the bulk metals copper, stainless steel and titanium. While surface texturing with nanosecond pulses is limited to feature sizes in the micrometer range, utilizing picosecond pulses can lead to sub-micrometer structures. The modelling and simulation of ps-DLIP is based on the two-temperature model and was carried out for a pulse duration of 35 ps at 515 nm wavelength and a laser fluence of 0.1 J/cm<sup>2</sup>. The subsurface temperature distribution of both electrons and phonons was computed for periodic line-like structures with a pitch of 0.8 μm. The increase in temperature rises for a lower absorption coefficient and a higher thermal conductivity. The distance, at which the maximum subsurface temperature occurs, increases for a small absorption coefficient. High absorption and low thermal conductivity minimize internal heating and give rise to a pronounced surface micro topography with pitches smaller than 1 μm. In order to confirm the computed results, periodic line-like surface structures were produced using two interfering beams of a Yb:YAG-Laser with 515 nm wavelength and a pulse duration of 35 ps. It was possible to obtain a pitch of 0.7 μm on the metallic surfaces.

**Keywords:** picosecond DLIP, surface structure, Two-temperature model

## 1. Introduction

Surface engineering is considered as an essential technology for many key industry sectors, e.g. automotive industry, “green” energy, life science, etc. It is also connected to a variety of social themes of the 21<sup>st</sup> century like climate, energy, mobility and healthcare. In order to meet the technical requirements to succeed in a specific market, it is necessary to develop and establish new manufacturing processes to produce smaller geometric structures on large areas.

Grooves, dimples and pillar-like structures can be generated with different technologies. Besides lithographic methods such as photolithography [1], interference lithography [2, 3], nanoimprint lithography [4, 5] and deep X-ray lithography [6], short (nanosecond and sub-nanosecond) and ultrashort pulsed (pico- and femtosecond) laser-based techniques have been established to fabricate well-defined surface micro pattern over the last decades [7-10]. The effect of such micro structures improves, for example, the anti-adhesive properties of cutting tools [11], reduces friction of automotive components [12, 13], generates hydrophobic or superhydrophobic surfaces [14-16], enhances cell proliferation on biomaterials [17-19], boosts solar cell efficiency [20] and promotes adhesive bonding [21].

Current lithographic techniques require expensive equipment, use hazardous materials and are time consuming due to serial processing, while laser techniques allow in contradiction a high level of flexibility. Both nanosecond- and sub-nanosecond pulsed laser systems in the range  $< 100$  ps have provided the opportunity to trigger specific material properties by impinging an engineered surface micro topography [22-26]. Although current direct laser writing systems are generally sufficient to produce microtopographies down to  $10 - 15 \mu\text{m}$ , they exhibit significant limitations with respect to process speed and feature sizes, especially below  $5 \mu\text{m}$ . An approach to generate periodic pattern with subwavelength feature sizes is known as LIPSS – laser induced periodic surface structures. At laser pulses below  $500$  fs, surface ripples develop on the surface after the irradiation of solid materials like semiconductors, insulators and metals [27-30]. LIPSS methods are currently limited to small area processing due to speed limitations. Also, period and complexity of the ripples are inconsistent across the ablation spot. Overall, the underlying physical mechanisms are not yet fully understood.

The interference of two or more coherent laser beams can be applied to produce periodic grooves, grids or dimples with pitches (periods) in the micrometer and sub-micrometer range on a variety of materials, such as metals, polymers and thin metallic films [31-33]. This technique is called direct laser interference patterning (DLIP). For the case of bulk metals, DLIP is based on a photothermal process that involves local melting and/or selective ablation at the interference maxima. For nanosecond laser pulses, the primary material removal mechanism is ablation but substantial melting occurs for metallic materials. The surface temperature is determined by thermal conductivity, thus laser ablation is an equilibrium process which obeys FOURIER'S law of heat conduction [34, 35]. The minimum achievable pitch is therefore limited by the thermal diffusion length, which is approximately  $1 \mu\text{m}$  for stainless steel and titanium, and  $2 \mu\text{m}$  for copper [36, 37]. When the laser pulse duration reduces to the order of picosecond or femtosecond, little thermal damage is observed and pitches below  $1 \mu\text{m}$  should be feasible. DLIP with sub-nanosecond laser pulses  $< 100$  ps offers therefore the possibility to fabricate precisely defined surface topographies with pitches in the sub-micron range. These sub-micrometer topographies can potentially be used to generate an additional specific surface function, such as antireflection or dirt-repellent effects.

In this study, DLIP is used to fabricate periodic grooves with pitches below  $1 \mu\text{m}$  on the bulk metals copper, stainless steel (type: 304), and titanium (TiAl6V4). The metals were chosen as the focus of this study due to their relevance to the industry, e.g. for medical applications (Cu, Ti), the printing industry (Cu, stainless steel) and the food industry (stainless steel). The patterning is achieved using a Yb:YAG laser system, where frequency doubled laser beams at  $515$  nm wavelength overlap to form an interference pattern with a peak-to-valley architecture. In addition, thermal simulation by finite element method (FEM) was carried out modelling the photothermal laser interactions. The two-temperature model (TTM) is considered for the first time to represent the heat transfer under picosecond DLIP. It describes the time-dependent excitation of the electrons and the subsequent energy transfer from the electrons to the phonons (lattice) in the metallic material. The temperature profiles of both electrons and phonons of bulk copper, iron (substitute for stainless steel) and titanium irradiated by a single-shot picosecond laser pulse are determined solving the one-dimensional differential equations according to the TTM. The temperature dependence of the thermal conductivity is taken into account and examined via FEM for copper.

## **2. Experimental**

### *2.1 Thermal Model*

When laser radiation strikes matter, the energy is partly reflected, transmitted or absorbed. In metals, the laser energy of an incident laser pulse is firstly absorbed by the electrons, leaving the phonons “cold” for an initial time period of femtoseconds [38]. The heat is subsequently transmitted by electron-phonon collisions. This energy exchange between electrons and phonons is characterized by the “relaxation time”, which describes the decrease of energy

upon the laser pulse until a thermal equilibrium between electrons and phonons is established, and can be described by the linear differential equations

$$c_i \frac{\partial T_i}{\partial t} = -c_e \frac{\partial T_e}{\partial t} = \gamma(T_e - T_i), \quad (1)$$

where  $t$  is the time,  $c_i$ ,  $c_e$  and  $T_i$ ,  $T_e$  are the specific heat capacity and temperature of the phonons and electrons, respectively. The parameter  $\gamma$  depends on the material, and describes the strength between the electron-phonon-coupling. Applying FOURIER'S law of heat conduction, two equations for the lattice and electron temperature can be derived. For the one-dimensional case ( $z$  is the direction perpendicular to the metal surface) they become [39]

$$c_e \frac{\partial T_e}{\partial t} = \frac{\partial}{\partial z} \kappa_e \frac{\partial T_e}{\partial z} - \gamma(T_e - T_i) + \alpha Q(z, t) \quad (2)$$

$$c_i \frac{\partial T_i}{\partial t} = \frac{\partial}{\partial z} \kappa_i \frac{\partial T_i}{\partial z} + \gamma(T_e - T_i). \quad (3)$$

The coefficients  $\kappa_e$  and  $\kappa_i$  are the thermal conductivity of the electrons and phonons,  $\alpha$  is the absorption coefficient of the material, and the source term  $Q(t, z)$  is associated to the energy of the laser pulse. Since the thermal conductivity of the electrons is considerably higher than the thermal conductivity of the photons, the heat conduction term in Eq. (3) can be neglected. While the electron heat capacity depends linearly from the electron temperature ( $c_e = c_{e0} T_e$ ,  $c_{e0}$ : electron heat capacity at room temperature), the heat capacity of the phonons is constant for temperatures higher than the DEBYE temperature [40]. In most cases, the system of heat equations (Eq. (2) and Eq. (3)) can only be solved numerically. However, there are approximations to find analytical solutions within a certain range.

The values of  $\kappa_e$  and  $\alpha$  depend on the temperature. According to the DRUDE model, the electron thermal conductivity of metals can be written as [41]

$$\kappa_e = \frac{1}{3} v^2 c_e \tau, \quad (4)$$

where  $v^2$  is the mean square electron speed. Both electron-electron (e-e)  $\tau_{ee}$  and electron-phonon (e-ph) scatterings  $\tau_{ep}$  contribute to the total scattering time  $\tau = \tau_{ee} + \tau_{ep}$ , where  $1/\tau_{ee} = AT_e^2$  and  $1/\tau_{ep} = BT_i$  [42]. The thermal conductivity then becomes

$$\kappa_e = \frac{1}{3} v_F^2 \gamma \frac{T_e}{BT_i + AT_e^2}, \quad (5)$$

where  $v_F$  is the FERMI velocity, and both  $A$  and  $B$  material dependent constants. When  $T_e$  remains smaller than the FERMI energy  $E_F$ , Eq. (5) can be approximated by

$$\kappa_e \approx \kappa_0 \frac{T_e}{T_i}, \quad (6)$$

where  $\kappa_0$  is the thermal conductivity at room temperature  $T_0 = 300$  K. If  $T_e$  is larger than the FERMI energy, Eq. (6) is no longer valid, and the following equation should be used [43]:

$$\kappa_e = C \frac{(\mathcal{G}^2 + 0.16)^{5/4} (\mathcal{G}^2 + 0.44) \mathcal{G}}{(\mathcal{G}^2 + 0.092)^{1/2} (\mathcal{G}^2 + b \mathcal{G}_i)}, \quad (7)$$

where  $\mathcal{G} = k_B T_e / E_F$ ,  $\mathcal{G}_i = k_B T_i / E_F$  ( $k_B$ : Boltzmann constant), and  $C$  and  $b$  are specific material parameters.

The energy intensity distribution of a line-like interference pattern (grooves) is considered

$$\Phi(x, y) = 4\Phi_0 \cos^2\left(kx \sin \frac{\theta}{2}\right) \text{ at } z = 0, \quad (8)$$

where  $\Phi_0$  is the laser fluence of each beam,  $\theta$  the angle of incidence between the interfering beams, and  $k = 2\pi / \lambda$  is the wave number at the laser wavelength  $\lambda$ . The temporal intensity distribution of the laser pulse follows a Gaussian distribution

$$I(x, y, t) = \frac{\Phi(x, y)}{\sigma\sqrt{2\pi}} \exp\left(-\frac{(t-t_0)^2}{2\sigma^2}\right) \quad (9)$$

with the standard deviation

$$\sigma = \frac{\tau_p}{2\sqrt{2\ln 2}}, \quad (10)$$

where  $t_0$  is the pulse arrival time, and  $\tau_p$  is the pulse duration of the laser (full width at half maximum FWHM). The absorbed heat source term at the metallic surface is given by the BEER-LAMBERT law

$$Q(x, z, t) = \alpha(1-R) \frac{\Phi(x)}{\sigma\sqrt{2\pi}} \exp\left(-\frac{(t-t_0)^2}{2\sigma^2} - \alpha z\right), \quad (11)$$

where  $R$  is the reflectivity of the material's surface.

The numerical analysis was performed using the software FlexPDE (Version 6.38). The material properties  $\alpha$  and  $c_i$  were considered independent from the temperature. The model neglects the latent heat of fusion and vaporization. Iron was used in the simulation since it is the primary element in stainless steel. The material parameter, which were used in the calculations are shown in Table 1.

**Table 1:** Optical and thermal constants at 300K used for the calculations.

		Copper	Iron	Titanium
$n$ :	Refractive index (at 515 nm)	1.18 <sup>[44]</sup>	2.86 <sup>[45]</sup>	2.44 <sup>[45]</sup>
$k$ :	Extinction coefficient (at 515 nm)	2.61 <sup>[44]</sup>	2.91 <sup>[45]</sup>	3.30 <sup>[45]</sup>
$R$ :	Reflectivity <sup>a</sup>	0.6	0.51	0.56
$\alpha$ :	Absorptivity <sup>b</sup> (1/m)	$6.4 \times 10^7$	$7.1 \times 10^7$	$8.05 \times 10^7$
$\kappa_0$ :	Electron thermal conductivity <sup>[46]</sup> (W/mK)	401	80.2	21.9
$c_{e0}$ :	Electron heat capacity (J/m <sup>3</sup> K <sup>2</sup> )	96.6 <sup>[47]</sup>	706.4 <sup>[48]</sup>	319.8 <sup>[49]</sup>
$c_i$ :	Phonon heat capacity <sup>[50]</sup> (J/m <sup>3</sup> K <sup>2</sup> )	$3.39 \times 10^6$	$3.5 \times 10^6$	$2.3 \times 10^6$
$\gamma$ :	Electron-Phonon-Coupling coefficient <sup>[46]</sup> (W/m <sup>3</sup> K <sup>1</sup> )	$25 \times 10^{16}$	$130 \times 10^{16}$	$260 \times 10^{16}$

<sup>a</sup> From  $R = \frac{(n-1)^2 + k^2}{(n+1)^2 + k^2}$

<sup>b</sup> From  $\alpha = 4\pi k / \lambda$

## 2.2 Direct laser interference patterning (DLIP)

Periodic pattern in the submicrometer regime were generated via interfering laser beams emitted by a pulsed Yb-YAG-Laser whose 1030 nm fundamental wavelength is frequency doubled to 515 nm at 35 ps pulse width. Figure 1a shows the interference setup. The incident beam is divided by a diffractive optical element (DOE) into two coherent beams of comparable intensities, collimated with a prism and finally recombined using an aspheric lens with a focal length of 60 mm. The interference of the two laser beam causes an intensity modulation, which is given by Eq. (8) and schematically shown in Fig. 1b. The angle of incidence defines the pitch  $p$  between two maxima or minima of the structure

$$p = \frac{\lambda}{2 \sin(\theta/2)}. \quad (12)$$

It is evident that the minimum possible pitch is 258 nm for  $\theta = 180^\circ$  ( $\lambda = 515$  nm). The structuring of the metallic samples (size: 10 x 10 mm<sup>2</sup>, thickness: 0.5 mm) was done by single exposure. The repetition frequency of the laser was 1 Hz. The irradiated samples were analyzed by means of scanning electron microscopy (SEM).

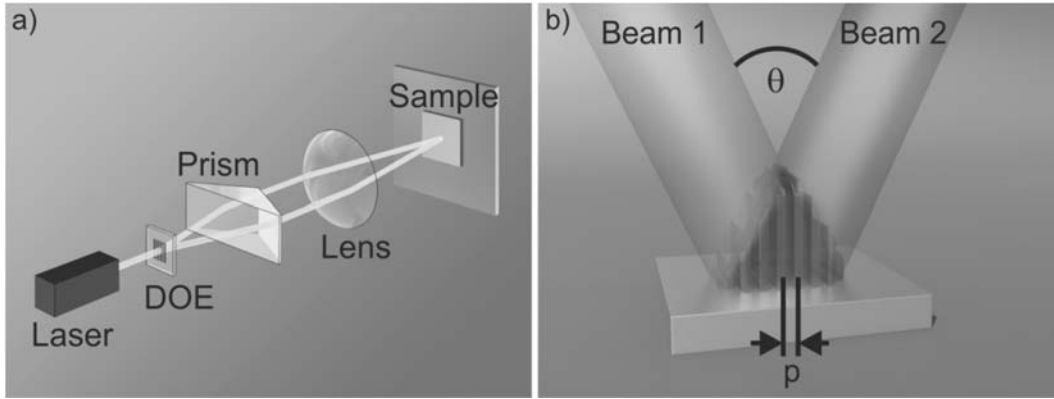


**Figure 1:** a) Experimental setup for the DLIP experiments; b) schematic of two interfering laser beams.

## 3. Results and Discussion

The TTM was used to model picosecond DLIP on the metals Cu, Fe and Ti. The influence of the temperature dependence of  $\kappa(T_e)$  is shown for copper in Fig. 2a, whereas the temperature of the lattice was assumed constant at  $T_0 = 300$  K. The thermal conductivity at room temperature  $\kappa_0 = 401$  W/mK as well as the parameters  $A = 1.75 \times 10^7$  1/sK and  $B = 1.98 \times 10^{11}$  1/sK<sup>2</sup> were taken from [46] and [51]. The parameters  $C = 386.5$  and  $b = 0.14$  in Eq. (7) result by comparing the coefficients  $A$  and  $B$  using Eq. (5) [52].

The thermal distribution of the subsurface temperature, which is characterized by  $T_e$  and  $T_i$ , can be calculated numerically for all cases of  $\kappa$  ( $\alpha$  is assumed constant). Figure 2b depicts both electron and phonon temperature on a copper surface after DLIP ( $p = 0.8 \mu\text{m}$ ) for a GAUSSIAN beam with a pulse duration of 1 ps, a fluence of 0.1 J/cm<sup>2</sup> and a center wavelength of 515 nm where the Eq. (5), (6) and (7) were applied and compared to the result of  $\kappa = \text{const.}$

The results in Fig. 2a indicate that Eq. (6) is only valid for  $T_e < 1000$  K. If the temperature increases, the thermal conductivity becomes rapidly too high. At temperatures  $T_e \approx 30000$  K ( $\approx 100 T_0$ ), Eq. (5) is no longer applicable because the values of  $\kappa$  become too small. It has also to be considered that the amount of radiant heat energy emitted by the surface increases as its temperature rises (STEFAN-BOLTZMAN law).

Computing the surface temperature of copper during laser radiation for  $\kappa = \text{const.}$  and Eq. (5) – (7) reveals a GAUSSIAN-like temperature distribution of  $T_e$  (Fig. 2b). The curves for

$\kappa = \text{const.}$  as well as Eq. (5) and Eq. (7) show a similar distribution. While the calculated results for Eq. (5) are slightly above of those of Eq. (7), the values of  $T_e$  for  $\kappa = \text{const.}$  appear below the solid line of Eq. (7). The graph following Eq. (6) underestimates the electron temperature significantly which shows good agreement with the according graph illustrated in Fig. 2a where the thermal conductivity increases at electron temperatures above 1000 K. Based on the results concerning the thermal conductivity that are shown in Fig. 2b, it appears reasonable to assume  $\kappa = \text{const.}$  for the FEM simulation.

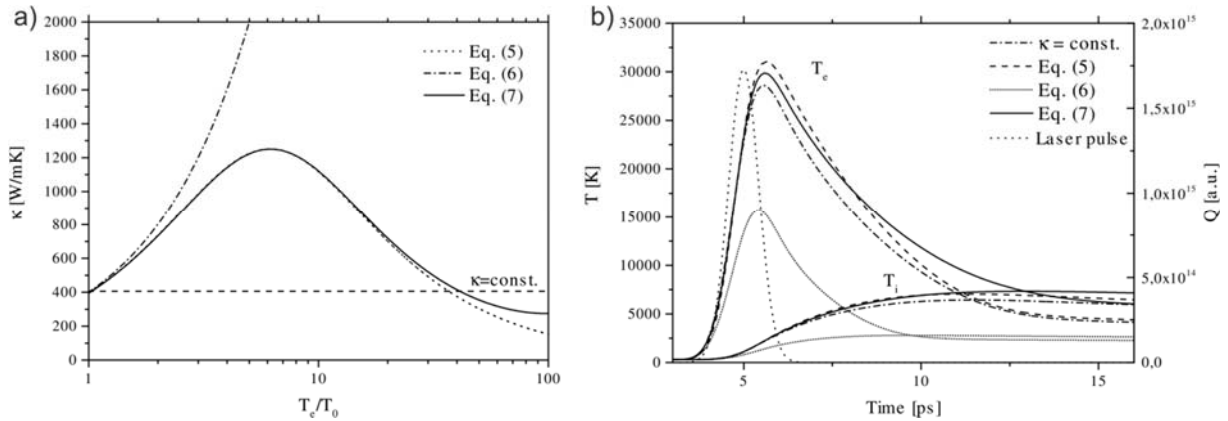


**Figure 2:** a) Thermal conductivity of the electrons in copper over the electron temperature applying Eq. (5), (6) and (7); b) electron ( $T_e$ ) and phonon temperature ( $T_i$ ) on a copper surface upon DLIP (wavelength: 515 nm, laser fluence:  $0.1 \text{ J/cm}^2$ ). The dotted line in b) shows the 1 ps GAUSSIAN pulse with  $Q$  being the intensity.

The surface temperature profiles shown in Fig. 3 are calculated from Eq. (2) and (3) using the copper (Cu), iron (Fe) and titanium (Ti) physical constants in Table 1, a fluence of  $0.1 \text{ J/cm}^2$  and a wavelength of 515 nm. For the heating pulse, a GAUSSIAN temporal profile with a pulse duration of 35 ps was assumed. All calculations were performed for a pitch of  $0.8 \mu\text{m}$ . The parameters were chosen for the TTM in very close proximity to the real values which were expected for the DLIP experiments.

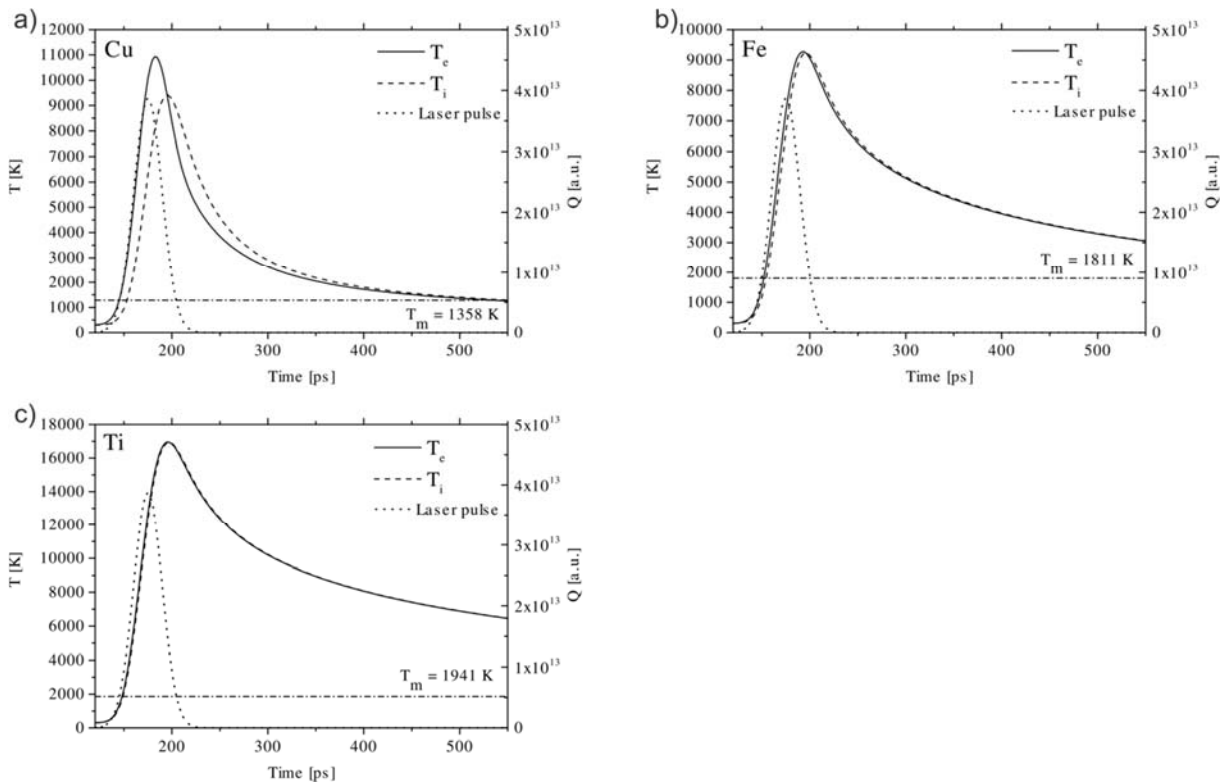


**Figure 3:** Computed temperature for a) copper (Cu); b) iron (Fe) and c) titanium (Ti) using a laser fluence of  $0.1 \text{ J/cm}^2$ . The surface electron temperature ( $T_e$ ) follows the solid line and the phonon temperature ( $T_i$ ) follows the dashed line. The dotted line shows the 35 ps GAUSSIAN pulse. The melting temperature ( $T_m$ ) for each material is also plotted (dash-dot line).

Qualitatively, it is found that the surface temperature follows the GAUSSIAN pulse shape for both electrons and phonons. Titanium exhibits the lowest thermal conductivity which explains the significant difference of the maximum temperature compared to copper and iron (Ti:  $T_{max} \approx 17000 \text{ K}$ , Fe:  $T_{max} \approx 9300 \text{ K}$ , Cu:  $T_{max} \approx 11000 \text{ K}$ ). For copper, the time shift between  $T_e$  and  $T_i$  shows  $\approx 10 \text{ ps}$  delay (Fig. 3a). This result can be explained by a rapid increase of the electron temperature at the beginning of the laser pulse, while the heat transfer from the electrons to the phonons occurs with a time delay which is in the order of the electron-phonon scattering time. Although the e-ph collision time in copper is given in the literature with  $\tau_{ep} = 240 \text{ ps}$  (at  $T_0 = 300 \text{ K}$ ) [53], a relaxation time in the order of a few picoseconds seems to be more reasonable. It can also be seen in Fig. 3a that the maximum phonon temperature ( $T_{i\ max} \approx 9400 \text{ K}$ ) is lower than the maximum electron temperature ( $T_{e\ max} \approx 11000 \text{ K}$ ) due to a higher heat capacity of the phonons. In addition, the plot shows that after  $\approx 15 \text{ ps}$ , when the highest phonon temperature is achieved,  $T_e$  drops below  $T_i$ . This can be attributed to the fact that the heat conduction cannot be compensated through e-ph coupling.

No considerable time shift between electron and phonon temperature is observed for iron ( $T_{e\ max} \approx T_{i\ max} \approx 9300 \text{ K}$ ) and titanium ( $T_{e\ max} \approx T_{i\ max} \approx 17000 \text{ K}$ ) (Fig. 3b and c). The heating pulse is evidently long compared to the e-ph scattering time and hence, electrons and phonons remain in thermal equilibrium. Thus, the non-equilibrium electron distribution is caused by a pulse width which is shorter than 35 ps. The critical pulse width for Cu, in which case non-thermal ablation can occur, appears in contradiction to Fe and Ti in the range of the utilized laser pulse length.

Figure 4 shows the temperature evolution as a function of depth in the materials after DLIP with a 35 ps laser pulse and the same laser fluence of  $0.1 \text{ J/cm}^2$ . The surface temperature distribution profiles were determined for the time  $\Delta t = t - t_0 = 35 \text{ ps}$  and a pitch of  $0.8 \mu\text{m}$  between two maxima and minima, respectively. The figure shows for each material that the laser-induced surface pattern can be distinguished. It is therefore apparent that using DLIP with picosecond laser pulses provides the ability to achieve pitches smaller than  $1 \mu\text{m}$  on metals. The observed heating effects depend strongly on the thermal properties of the material, namely the absorption coefficient and the thermal conductivity (see Table 1). Figure 4a – c shows a subsurface temperature at the intensity maxima of  $3800 \text{ K}$  for copper,  $8000 \text{ K}$  for iron and  $12500 \text{ K}$  for titanium. The increase in temperature is evidently greater at smaller values of the absorption coefficient and higher values of the thermal conductivity (larger absorption depth). Also, the distance, at which the maximum subsurface temperature occurs, increases with decreasing absorption coefficient. It is concluded that high absorption and low thermal conductivity, respectively, minimize the internal heating effects and give rise to a more pronounced surface micro topography.

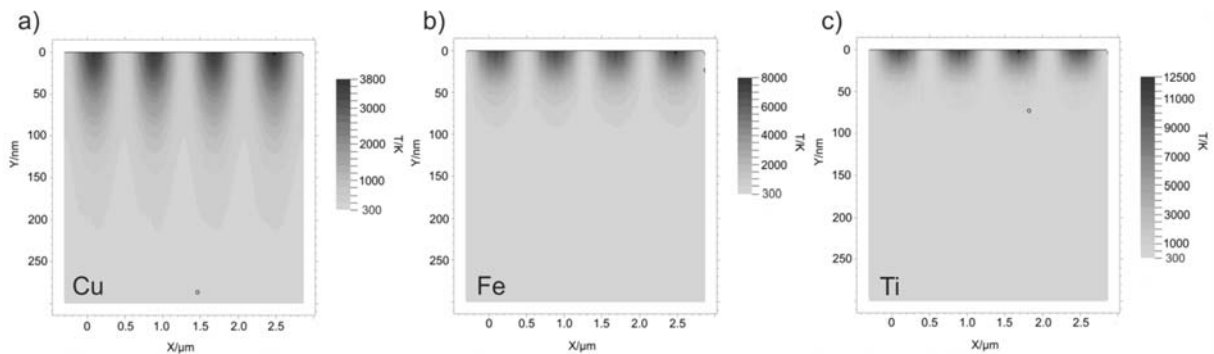


**Figure 4:** Thermal absorption depth due to laser irradiation over the surface at  $\Delta t = 35 \text{ ps}$ : a) copper; b) iron and c) titanium. The pitch was  $0.8 \mu\text{m}$  at  $0.1 \text{ J/cm}^2$  laser fluence.

The temperature difference between a minima and a maxima was calculated to  $\sim 3000$  K (Cu),  $\sim 6000$  K (Fe) and  $\sim 12000$  K (Ti), respectively. In fact, the temperature values at the intensity minima remain below the melting point ( $T_m(\text{Cu}) = 1358$  K,  $T_m(\text{Fe}) = 1811$  K,  $T_m(\text{Ti}) = 1941$  K). After  $\Delta t = 425$  ps, the subsurface temperature drops to 1000 K (Cu), 3100 K (Fe) and 6600 K (Ti) (Fig. 5). The surface cools down by the conduction of heat inside the material, whereas the thermal penetration depth depends clearly on the thermal heat conduction of the material. Copper provides a much better heat dissipation than iron and titanium. The electron-phonon-coupling of Cu is weaker compared to Fe and Ti (see values of  $\gamma$  in Table 1), thus its electrons can transport the heat much more efficiently. The temperature difference between maxima and minima decreases to  $\sim 200$  K (Cu) (Fig. 5a),  $\sim 2700$  K (Fe) (Fig. 5b) and  $\sim 5800$  K (Ti) (Fig. 5c). The plots also indicate that the melting temperature of each metal is not exceeded at the minima, despite a time period of  $\Delta t > 10 \tau_p$ . This provides further evidence for the fabrication of a pitch smaller than  $1 \mu\text{m}$  on metallic surfaces using DLIP.

Another effect that contributes to creating surface pattern with small pitches includes the thermal diffusion length  $l_T = (\kappa_D \tau_p)^{1/2}$ . The thermal diffusivity  $\kappa_D$  is given by  $\kappa_D = \kappa_0 / \rho c_p$ , being  $\kappa_0$  the thermal conductivity,  $\rho$  the density and  $c_p$  the specific heat capacity. The thermal diffusion length indicates the smallest pitch that can be obtained with DLIP on metallic surfaces by approximating it with  $p_{min} \approx 2l_T$  [36]. Thus, the theoretical minimum pitch can be correlated to the laser pulse width as well as the thermal properties of the metal and gives  $p_{min} \approx 130$  nm (Cu), 60 nm (Fe) and 40 nm (Ti) ( $\tau_p = 35$  ps). However, from Eq. (12) we conclude that the minimum feasible value is  $p_{min} \approx \lambda/2 \approx 260$  nm.

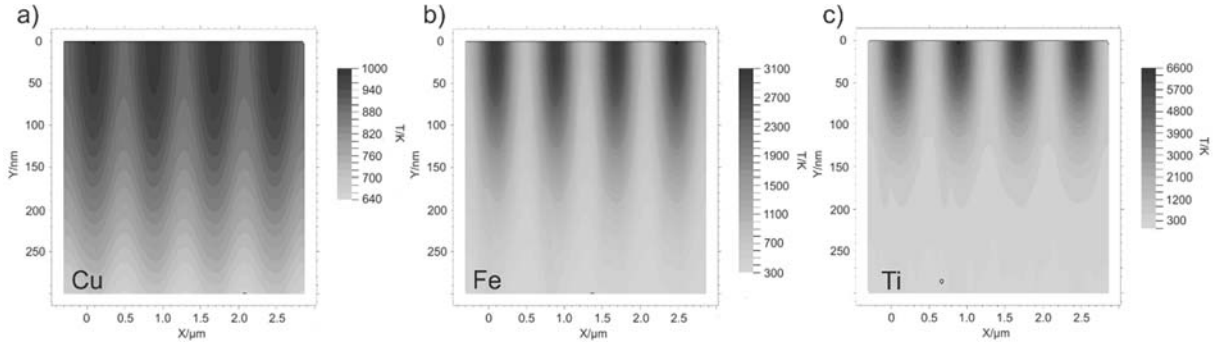


**Figure 5:** Thermal absorption depth due to laser irradiation over the surface at  $\Delta t = 425$  ps: a) copper; b) iron and c) titanium. The pitch was  $0.8 \mu\text{m}$  at  $0.1 \text{ J/cm}^2$  laser fluence.

In order to evaluate the possibility of fabricating sub-micrometer structures using DLIP, surface of copper, stainless steel and titanium were irradiated at a pulse duration of 35 ps and a wavelength of 515 nm. The experiments were conducted using both a single shot and two consecutive laser pulses. A pitch of  $\sim 0.7 \mu\text{m}$  between two maxima (or minima) was chosen. With an appropriate laser fluence of  $1.6 \text{ J/cm}^2$  (copper),  $1.3 \text{ J/cm}^2$  (stainless steel) and  $0.9 \text{ J/cm}^2$  (titanium), line-like structures with good quality were produced.

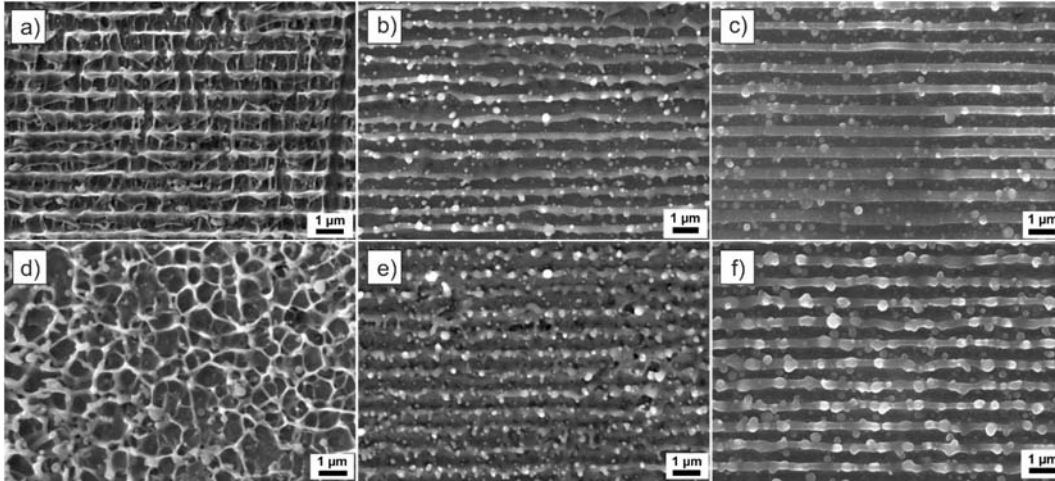


**Figure 6:** Periodic line-like structure upon DLIP with a pulse duration of 35 ps and a wavelength of 515 nm on a) Cu, single pulse at 1.6 J/cm<sup>2</sup>; b) stainless steel, single pulse at 1.3 J/cm<sup>2</sup>; c) Ti, single pulse at 0.9 J/cm<sup>2</sup>; d) Cu, two pulses at 1.6 J/cm<sup>2</sup> for each pulse; e) stainless steel, two pulses at 1.3 J/cm<sup>2</sup> for each pulse; f) Ti, two pulses at 0.9 J/cm<sup>2</sup> for each pulse.

For one laser pulse there are distinct maxima and minima regions (Fig. 6a – c). However, the copper, the stainless steel and the titanium surfaces melt during the pulse duration of the laser. After applying two consecutive laser pulses with equal fluence and a temporal delay of 1 s, the quality of the microstructures deteriorates (Fig. 6d – f). While visible patterns are still obtained for both stainless steel and titanium, the structured copper surface appears much less defined. Copper has a lower melting point than stainless steel and titanium, creating a larger melt puddle. It is generally assumed that the reflectivity decreases upon the first laser pulse which results in a higher absorption of the second pulse and an increased amount of molten material due to higher temperatures. Consequently, the quality of the micro surface pattern decreases.

The experimental results are consistent with the predictions from the numerical simulation (Fig. 7). Higher temperatures at both maxima and minima compared to Fig. 4 can be explained by the larger laser fluence (0.1 J/cm<sup>2</sup> vs. 0.9 J/cm<sup>2</sup> (Ti), 1.3 J/cm<sup>2</sup> (Fe) and 1.6 J/cm<sup>2</sup> (Cu)). However, the temperature at the minima does not exceed the melting point for Cu, Fe and Ti and the 0.7 μm pitch can still clearly be distinguished. This result is consistent with the micrographs for a single pulse in Fig. 6a - c. The utilized pulse duration of 35 ps caused significantly less melting compared to pulse durations in the range of nanoseconds [37], but it is insufficient to provide the required laser intensity for a “cold” type ablation. It is indicated by the computer simulation (see Fig. 3) that 35 ps is longer than the e-ph scattering time, i.e. the patterning process is characterized by a photo-thermal response. The laser processing of the investigated metals can therefore be treated on the basis of the classical theory of heat conduction.

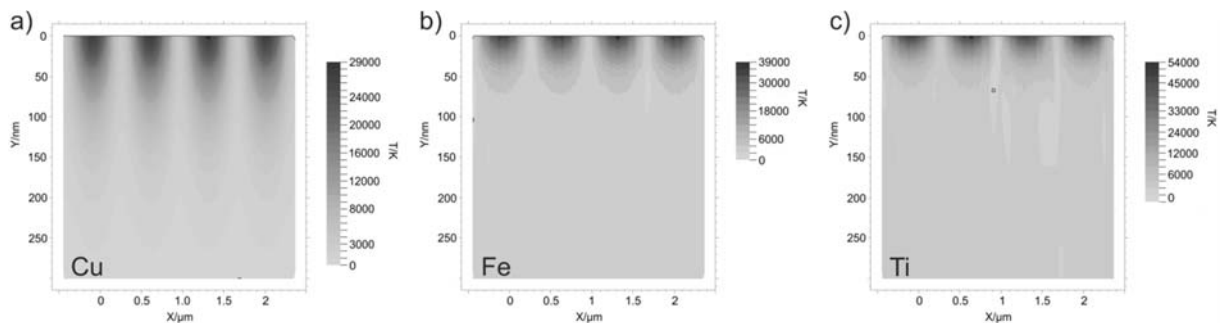


**Figure 7:** Thermal response after laser irradiation over the surface at  $\Delta t = 35$  ps: a) copper (laser fluence: 1.6 J/cm<sup>2</sup>); b) iron (laser fluence: 1.3 J/cm<sup>2</sup>) and c) titanium (laser fluence: 0.9 J/cm<sup>2</sup>). The pitch was 0.7 μm.

## 4. Conclusion

The thermal effects of pulsed picosecond DLIP were simulated by the solution of a system of two differential equations for bulk copper, stainless steel and titanium. The temperature-dependence of the thermal conductivity was taken into account. The calculated results have shown that the thermal conductivity can be kept constant over the investigated temperature range. The subsurface temperature curves were computed for both electrons and phonons in titanium, iron (substitute for stainless steel) and copper with a pitch of 0.8  $\mu\text{m}$ . For a pulse duration of 35 ps and a fluence of 0.1 J/cm<sup>2</sup> Cu exhibits a slight delay between electron and phonon temperature, while Fe and Ti remain in thermal equilibrium.

The subsurface temperature evolution showed a strong dependence on the thermal properties of the material, in particular the absorption coefficient and the thermal conductivity. The highest temperature at the intensity maxima varies among the metals up to 3800 K for copper, 8000 K for iron and 12500 K for titanium. After  $\Delta t = 425$  ps, the according temperature decreases to a maximum of 1000 K (Cu), 3100 K (Fe) and 6600 K (Ti). This effect can be explained by the thermal conductivity of copper. A key factor for the DLIP process is that the temperature remains below the melting point at the intensity minima. In addition, the thermal diffusion length determines the minimal achievable pitch with values of 130 nm (Cu), 60 nm (Fe) and 40 nm (Ti). From these considerations, it was predicted that pitches smaller than 1  $\mu\text{m}$  at a wavelength of 515 nm can be fabricated.

The confirmation of the numerical analysis was provided through experiments with two interfering laser beams irradiated by using a pulsed Yb-YAG-Laser at a wavelength of 515 nm and a pulse duration of 35 ps on copper, stainless steel and titanium surfaces. It was shown that pitches of approximately 0.7  $\mu\text{m}$  can be achieved with a laser fluence of 1.6 J/cm<sup>2</sup> (Cu), 1.3 J/cm<sup>2</sup> (Fe) and 0.9 J/cm<sup>2</sup> (Ti). Well shaped line-like surface structures were obtained for single laser pulses, while the quality decreases slightly for double pulse irradiation. The experimental results show that melting still has a predominant effect on the pattern formation, if a pulse duration of 35 ps is utilized. Interesting is the opportunity to investigate DLIP utilizing a pulse duration between 5 and 10 ps to achieve non-thermal ablation. In addition, experiments with a wavelength of 257 nm can be conducted. This could potentially allow pitches below 0.5  $\mu\text{m}$  on metallic surfaces.

## Acknowledgements

This research was funded by the German Federal Ministry of Economics and Energy (BMWi) within the Promotion of Joint Industrial Research Programme (IGF) due to a decision of the German Bundestag. It was part of the research project 18359BR by the Association for Research in Precision Mechanics, Optics and Medical Technology (F.O.M.) under the auspices of the German Federation of Industrial Research Associations (AiF).

This work was also supported by the German Research Foundation (DFG) through the Excellence Initiative by the German federal and state governments to promote top-level research at German universities (Grant No.: F-003661-553-41A-1132104).

## References

- [1] A. Gombert, B. Bläsi, The Moth-Eye Effect – From Fundamentals to Commercial Exploitations, in: E.A. Favret, N.O. Fuentes (Eds.), Functional Properties of Bio-Inspired Surfaces: Characterization and Technological Applications”, World Scientific Publishing Co. Pte. Ltd., Singapore, 2009, pp. 93-96.
- [2] H. Korre, C. P. Fucetola, J. A. Johnson, K. K. Berggren, Development of a simple, compact, low-cost interference lithography system, J. Vac. Sci. Technol. B 28 (2010) 20-24.
- [3] I. Byun, J. Kim, Cost-effective laser interference lithography using a 405 nm AlInGaN semiconductor laser, J. Micromech. Microeng. 20 (2010) 055024-055029.

- [4] U. Plachetka, M. Bender, A. Fuchs, B. Vratzov, T. Glinsner, F. Lindner, H. Kurz, Wafer scale patterning by soft UV-Nanoimprint Lithography, *Microelec. Eng.* 73-74 (2004) 167-171.
- [5] N. Koo, M. Bender, U. Plachetka, A. Fuchs, T. Wahlbrink, J. Bolten, H. Kurz, Improved mold fabrication for the definition of high quality nanopatterns by soft UV-Nanoimprint lithography using diluted PDMS material, *Microelec. Eng.* 84 (2007), 904-908.
- [6] C. Luo, Y. Li, S. Susumu, Fabrication of high aspect ratio subwavelength gratings based on X-ray lithography and electron beam lithography, *Optics & Laser Technology* 44 (2012) 1649-1653.
- [7] B. Tan, N. R. Sivakumar, K. Venkatakrishnan, Direct grating writing using femtosecond laser interference fringes formed at the focal point, *J. Opt. A: Pure Appl. Opt.* 7 (2005) 169–174.
- [8] X. Wang, F. Chen, H. Liu, W. Liang, Q. Yang, J. Si, X. Hou, Fabrication of micro-gratings on Au–Cr thin film by femtosecond laser interference with different pulse durations, *Appl. Surf. Sci.* 255 (2009) 8483–8487.
- [9] J.-H. Klein-Wiele, P. Simon, Fabrication of periodic nanostructures by phase-controlled multiple-beam interference, *Appl. Phys. Lett.* 83 (2003), 4707-4709.
- [10] S. Matsuo, S. Juodkazis, H. Misawa, Femtosecond laser microfabrication of periodic structures using a microlens array, *Appl. Phys. A* 80 (2005) 683–685.
- [11] T. Enomoto, T. Sugihara, Improving anti-adhesive properties of cutting tool surfaces by nano-/micro-textures, *CIRP Ann.-Manuf. Techn.* 59 (2010) 597–600.
- [12] I. Etsion, E. Sher, Improving fuel efficiency with laser surface textured piston rings, *Tribol. Int.* 42 (2009) 542–547.
- [13] A. Ronen, I. Etsion, Y. Kligerman, Friction-Reducing Surface-Texturing in Reciprocating Automotive Components, *Tribol. T.* 44 (2001), 359-366.
- [14] X. Hao, L. Wang, D. Lv, Q. Wang, L. Li, N. He, B. Lu, Fabrication of hierarchical structures for stable superhydrophobicity on metallic planar and cylindrical inner surfaces, *Appl. Surf. Sci.* 325 (2015) 151–159.
- [15] A. D. Sommers, A. M. Jacobi, Creating micro-scale surface topology to achieve anisotropic wettability on an aluminum surface, *J. Micromech. Microeng.* 16 (2006) 1571–1578.
- [16] B.H. Luo, P.W. Shum, Z.F. Zhou, K.Y. Li, Preparation of hydrophobic surface on steel by patterning using laser ablation process, *Surf. Coat. Tech.* 204 (2010) 1180–1185.
- [17] J. Tan, W. M. Saltzman, Biomaterials with hierarchically defined micro- and nanoscale structure, *Biomaterials* 25 (2004) 3593–3601.
- [18] E. Martínez, E. Engel, J.A. Planell, J. Samitier, Effects of artificial micro-andnano-structured surfaces on cell behavior, *Ann. Anat.* 191 (2009) 126-135.
- [19] L. Scheideler, J. Geis-Gerstorfer, D. Kern, F. Pfeiffer, F. Rupp, H. Weber, H. Wolburg, Investigation of cell reactions to microstructured implant surfaces, *Mater. Sci. Eng. C* 23 (2003) 455–459.

- [20] B. Liao, A. G. Aberle, T. Mueller, L. K. Verma, A. J. Danner, H. Yang and C. S. Bhatia, Ultrafine and High Aspect Ratio Metal Lines by Electron Beam Lithography for Silicon Solar Cell Metallisation, *Energy Procedia* 15 (2012) 91-96.
- [21] T. Schiefer, I. Jansen, M. Bieda, J.-S. Pap, A. F. Lasagni, Large Area Surface Structuring by Direct Laser Interference Patterning for Adhesive Bonding Applications, *Special Issue on WCARP-V 51* (2015) 223-224.
- [22] C. H. Crouch, J. E. Carey, J. M. Warrender, M. J. Aziz, E. Mazur, F. Y. Génin, Comparison of structure and properties of femtosecond and nanosecond laser-structured silicon, *Appl. Phys. Lett.* 84 (2004) 1850-1852.
- [23] J. Byskov-Nielsen, P. Balling, Laser structuring of metal surfaces: Micro-mechanical interlocking, *Appl. Surf. Sci.* 255 (2008) 5591-5594.
- [24] B.N. Chichkov, C. Momma, S. Nolte, F. von Alvensleben, A. Tünnermann, Femtosecond, picosecond and nanosecond laser ablation of solids, *Appl. Phys. A. Mater. Sci. Process.* 63 (1996) 109-115.
- [25] H. K. Tönshoff, C. Momma, A. Ostendorf, S. Nolte, and G. Kamlage, Microdrilling of metals with ultrashort laser pulses, *J. Laser Appl.* 12 (2000) 23-27.
- [26] S. Döring, A. Ancona, S. Hädrich, J. Limpert, S. Nolte, A. Tünnermann, Microdrilling of metals using femtosecond laser pulses and high average powers at 515 nm and 1030 nm, *Appl. Phys. A. Mater. Sci. Process.* 100 (2010) 53-56.
- [27] V. Oliveira, S. Ausset, R. Vilar, Surface micro/nanostructuring of titanium under stationary and non-stationary femtosecond laser irradiation, *Appl. Surf. Sci.* 255 (2008) 7556-7560.
- [28] A. Y. Vorobyev, C. Guo, Multifunctional surfaces produced by femtosecond laser pulses, *J. Appl. Phys.* 117 (2015), 033103-033103-5.
- [29] J. Bonse, J. Krüger, Pulse number dependence of laser-induced periodic surface structures for femtosecond laser irradiation of silicon, *J. Appl. Phys.* 108 (2010) 034903-034903-5.
- [30] R. Le Harzic, D. Dörr, D. Sauer, F. Stracke, H. Zimmermann, Generation of high spatial frequency ripples on silicon under ultrashort laser pulses irradiation, *Appl. Phys. Lett.* 98 (2011), 211905-211905-3.
- [31] M. Bieda, C. Schmädicke, A. Wetzig, A. F. Lasagni, Direct Laser Interference Patterning of Planar and Non-Planar Steels and their Microstructural Characterization, *Met. Mater. Int.* 19 (2013) 81-86.
- [32] M. F. Broglia, D. F. Acevedo, D. Langheinrich, H. R. Perez-Hernandez, C. A. Barbero, A. F. Lasagni, Rapid Fabrication of Periodic Patterns on Poly(styrene-co-acrylonitrile) Surfaces using Direct Laser Interference Patterning, *Int. J. Polymer Sci.* 2015 (2015) 7pp.
- [33] S. Indrišiūnas, B. Voisiat, M. Gedvilas, G. Račiukaitis, Two complementary ways of thin-metal-film patterning using laser beam interference and direct ablation, *J. Micromech. Microeng.* 23 (2013) 9pp.
- [34] F. Mücklich, A. F. Lasagni, C. Daniel, Laser interference metallurgy-periodic surface patterning and formation of intermetallics, *Intermetallics* 13 (2005) 437-442.

- [35] C. Demuth, M. Bieda, A. F. Lasagni, A. Mahrle, A. Wetzig, E. Beyer, Thermal simulation of pulsed direct laser interference patterning of metallic substrates using the smoothed particle hydrodynamics approach, *J. Mat. Process. Tech.* 212 (2012) 689-699.
- [36] A. F. Lasagni, M. D'Allessandria, R. Giovanelli, F. Mücklich, Advanced Design of Periodical Architecture in Bulk Metals by Means of Laser Interference Metallurgy, *Appl. Surf. Sci.* 254 (2007) 930-936.
- [37] M. Bieda, E. Beyer, A. F. Lasagni, Direct fabrication of hierarchical microstructures on metals by means of direct laser interference patterning, *J. Eng. Mater. Technol* 132 (2010) 031015-031015-6.
- [38] B. Rethfeld, A. Kaiser, M. Vicanek, G. Simon, Ultrafast dynamics of nonequilibrium electrons in metals under femtosecond laser irradiation, *Phys. Rev. B* 65 (2002) 214303-214303-11.
- [39] S. I. Anisimov, B. L. Kapeliovich, T. L. Perel'man, Electron emission from metal surfaces exposed to ultrashort laser pulses, *Zh. Eksp. Teor. Fiz.* 66 (1974) 776-781.
- [40] S. I. Anisimov, B. S. Luk'yanchuk, Selected problems of laser ablation theory, *Physics - Uspekhi* 45 (2002) 293-324.
- [41] N. W. Ashcroft, N. D. Mermin, *Solid State Physics*, College ed., Harcourt College Publishers, 1976.
- [42] X.Y. Wang, D.M. Riffe, Y.-S. Lee, M.C. Downer, Time-resolved electron-temperature measurement in a highly excited gold target using femtosecond thermionic emission, *Phys. Rev. B* 50 (1994) 8016-8019.
- [43] S. I. Anisimov, B. Rethfeld, On the Theory of Ultrashort Laser Pulse Interaction with a Metal, *Proc. SPIE - Int. Soc. Opt. Eng.* 3093 (1996) 192-203.
- [44] P.B. Johnson, R.W. Christy, Optical Constants of the Noble Metals, *Phys. Rev. B* 6 (1972) 4370-4379.
- [45] P.B. Johnson, R.W. Christy, Optical constants of transition metals: Ti, V, Cr, Mn, Fe, Co, Ni, and Pd, *Phys. Rev. B* 9. (1974) 5056-5069.
- [46] Z. G. Wang, C. Dufourt, E. Paumiert, M. Toulemoude, The  $S_e$  sensitivity of metals under swift-heavy-ion irradiation: a transient thermal process, *J. Phys. Condens. Matter* 6 (1994) 6733-6750.
- [47] L. Yang, C.-Y. Wang, W. Yang, Numerical Simulation and Analysis on 3D Temperature Field of the Metal Ablated with Femtosecond Pulse Laser, 3rd International Photonics & OptoElectronics Meetings (POEM 2010), *Journal of Physics: Conference Series* 276 (2011) 012032.
- [48] R. Hummel, *Electronic Properties of Materials*, third ed., Springer, New York, 2000.
- [49] R. R. Rao, A. Rajput, Lattice specific heat and thermal expansion of titanium, *Phys. Rev. B* 19 (1979) 3323-3328.
- [50] E. Majchrzak, J. Poteralska, Two-Temperature Microscale Heat Transfer Model Part II: Determination of Lattice Parameters, *Scientific Research of the Institute of Mathematics and Computer Science* 9 (2010) 109-120.

[51] D. Zhang, L. Guan, Laser Ablation, in: S. Hashmi (Ed.), *Comprehensive Materials Processing*, Elsevier, Amsterdam, 2014, pp. 125-169.

[52] C. Schäfer, H. M. Urbassek, L. V. Zhigilei, Metal ablation by picosecond laser pulses: A hybrid simulation, *Phys. Rev. B* 66 (2002) 115404-115404-8.

[53] G.L. Eesley, Generation of nonequilibrium electron and lattice temperatures in copper by picosecond laser pulses, *Phys. Rev. B* 33 (1986) 2144-2152.